

## Giant magnetoelectric effect in negative magnetostrictive/piezoelectric/positive magnetostrictive semiring structure

Lingyu Zeng, Minhong Zhou, Ke Bi, and Ming Lei

Phone number Lingyu Zeng 15510717609

Citation: *Journal of Applied Physics* **119**, 034102 (2016); doi: 10.1063/1.4940382

View online: <http://dx.doi.org/10.1063/1.4940382>

View Table of Contents: <http://scitation.aip.org/content/aip/journal/jap/119/3?ver=pdfcov>

Published by the [AIP Publishing](#)

---

### Articles you may be interested in

[Resonance magnetoelectric effect in Ni/Pb\(Zr,Ti\)O<sub>3</sub>/Terfenol-D trilayered composites with different mechanical boundary conditions](#)

*Appl. Phys. Lett.* **104**, 252411 (2014); 10.1063/1.4885515

[Effect of magnetic domain structure on longitudinal and transverse magnetoelectric response of particulate magnetostrictive-piezoelectric composites](#)

*Appl. Phys. Lett.* **104**, 112903 (2014); 10.1063/1.4869304

[The effects of interface misfit strain and surface tension on magnetoelectric effects in layered magnetostrictive-piezoelectric composites](#)

*J. Appl. Phys.* **114**, 044109 (2013); 10.1063/1.4816693


[Enhancement of magnetoelectric coupling in a piezoelectric-magnetostrictive semiring structure](#)

*J. Appl. Phys.* **106**, 126101 (2009); 10.1063/1.3271140

[Magnetoelectric characteristics of a dual-mode magnetostrictive/piezoelectric bilayered composite](#)

*Appl. Phys. Lett.* **92**, 072903 (2008); 10.1063/1.2840177

---


**SHIMADZU**  
Excellence in Science

## Powerful, Multi-functional UV-Vis-NIR and FTIR Spectrophotometers

Providing the utmost in sensitivity, accuracy and resolution for applications in materials characterization and nano research

- Photovoltaics
- Polymers
- Thin films
- Paints
- Ceramics
- DNA film structures
- Coatings
- Packaging materials

[Click here to learn more](#)



# Giant magnetoelectric effect in negative magnetostrictive/piezoelectric/positive magnetostrictive semiring structure

Lingyu Zeng, Minhong Zhou, Ke Bi,<sup>a)</sup> and Ming Lei<sup>a)</sup>

State Key Laboratory of Information Photonics and Optical Communications & School of Science, Beijing University of Posts and Telecommunications, Beijing 100876, China

(Received 11 December 2015; accepted 9 January 2016; published online 21 January 2016)

Magnetoelectric (ME) Ni/PZT/TbFe<sub>2</sub> and TbFe<sub>2</sub>/PZT composites with two semiring structures are prepared. The dependence between ME coupling and magnetostrictive property of the composite is discussed. Because Ni possesses negative magnetostrictive property and TbFe<sub>2</sub> shows positive magnetostrictive property, the ME voltage coefficient of Ni/PZT/TbFe<sub>2</sub> semiring structure is much larger than that of TbFe<sub>2</sub>/PZT. In these composites, the ME voltage coefficient increases and the resonance frequency gradually decreases with the increase of the semiring radius, showing that structural parameters are key factors to the composite properties. Due to the strong ME coupling effect, a giant ME voltage coefficient  $\alpha_E = 44.8 \text{ V cm}^{-1} \text{ Oe}^{-1}$  is obtained. This approach opens a way for the design of ME composites with giant ME voltage coefficient.

© 2016 AIP Publishing LLC. [<http://dx.doi.org/10.1063/1.4940382>]

## I. INTRODUCTION

Magnetoelectric (ME) composites have attracted considerable attention due to their important applications, such as magnetic field sensors and tunable frequency devices.<sup>1–3</sup> The ME effect in ME composites can be defined as a coupling magnetic-mechanical-dielectric behavior. When a magnetic field is applied to such a structure, the ferromagnetic layer produces magnetostrictive effect, then the resulted strain is passed along to the piezoelectric phase, resulting in an electric polarization.<sup>4</sup> In order to enhance the ME coupling, rectangular and cylindrical structures were usually studied.<sup>5–8</sup> For most of the investigations, the classical mode is constructed layer by layer through interface bonding.<sup>9–12</sup> Hence, the ME effect is strongly related to the interface condition.<sup>13</sup>

In the past few years, lots of efforts have been paid on the design of new coupling mechanism to obtain a large ME coefficient.<sup>14–16</sup> Zhang *et al.*<sup>17</sup> reported a giant ME coefficient by introducing a semiring structure of lead zirconate titanate (PZT) with a positive magnetostrictive (Terfenol-D) insert based on bending mode. Our group also proposed a ME arc shaped structure that consisted of negative magnetostrictive layer (Ni) and PZT to realize the large ME coefficient.<sup>18</sup> Based on these studies, a negative magnetostrictive/piezoelectric/positive magnetostrictive semiring structure, which has rarely been reported so far, is expected to possess a giant ME effect. In this work, we report a giant magnetoelectric effect in negative magnetostrictive/piezoelectric/positive magnetostrictive semiring structure. Compared to the normal positive magnetostrictive/piezoelectric semiring structures, negative magnetostrictive/piezoelectric/positive magnetostrictive semiring structure shows a stronger ME coupling.

## II. EXPERIMENTAL DETAILS

The negative magnetostrictive, piezoelectric, and positive magnetostrictive materials used in this method are Ni, PZT, and TbFe<sub>2</sub>, respectively. PZT was cut into a semiring with the parameters of 1 mm in thickness and 5 mm in width. The inner radius  $R_1$  are 10.5 mm, 11.0 mm, 11.5 mm, 12.0 mm, and 12.5 mm, and the corresponding outer radius  $R_2$  are 11.5 mm, 12.0 mm, 12.5 mm, 13.0 mm, and 13.5 mm, respectively. The negative magnetostrictive material Ni was electroless deposited onto the outer surface of the PZT semiring. Pretreatment process including roughening, sensitization, activation, and reduction was applied prior to the electroless Ni deposition. Then, the PZT samples were bathed in a nickel sulfate solution to get the Ni deposition layer. The composition of the solution and operation parameters were described in detail elsewhere.<sup>19,20</sup> In this experiment, the thickness of the Ni layer was approximately 100  $\mu\text{m}$  and identical for all the ME structures. A TbFe<sub>2</sub> slab of 5 mm in width and 3 mm in thickness was fitted across the inner diameter of the semiring and cemented with epoxy. Both ends of the TbFe<sub>2</sub> insert that closest to the ring were machined to fit the semiring. The geometry arrangement of the Ni/PZT/TbFe<sub>2</sub> semiring structure is illustrated in Fig. 1.  $R = (R_1 + R_2)/2$  is the average radius of the PZT semiring. It was poled in an electric field in the radial direction.

The linear magnetostrictions of Ni and TbFe<sub>2</sub> were measured using standard strain-gauge technique in directions parallel ( $\lambda_{//}$ ) to the applied magnetic fields at room temperature. The ME effect of the Ni/PZT/TbFe<sub>2</sub> semiring structures was measured by applying both constant ( $H_{dc}$ ) and alternating ( $\delta H$ ) magnetic fields parallel to the length direction of the TbFe<sub>2</sub> insert. The induced voltage signal  $\delta V$  across the sample was applied with a power supply, amplified, and measured by an oscilloscope. The ME voltage coefficient was calculated using  $\alpha_E = \delta V / (t_{PZT} \delta H)$ , where  $t_{PZT}$  is the thickness of PZT layer and  $\delta H$  is the superimposed ac

<sup>a)</sup>Authors to whom correspondence should be addressed. Electronic addresses: bike@bupt.edu.cn and mlei@bupt.edu.cn

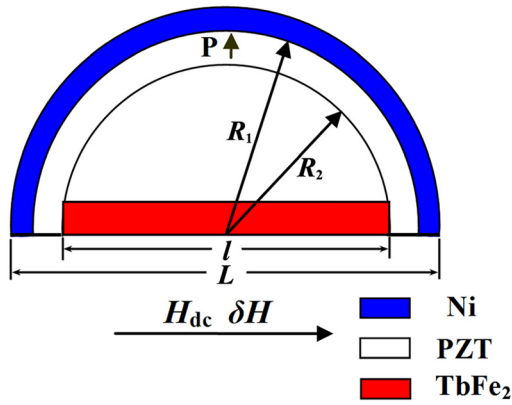


FIG. 1. Schematic geometry arrangement of the Ni/PZT/TbFe<sub>2</sub> semiring structure.

magnetic field that generated by Helmholtz coils. In this experiment,  $\delta H = 1.2$  Oe and the amplitude of the ac current through the coil is kept at 1 A.<sup>21</sup>

### III. RESULTS AND DISCUSSION

In order to figure out the ME coupling in the semiring structures, we first investigated the magnetostrictive properties of Ni and TbFe<sub>2</sub> layers separately. Figure 2 shows the representative data on the in-plane parallel magnetostriction  $\lambda_{//}$  versus applied magnetic field  $H$ . It is obvious that Ni has a negative magnetostriction, while TbFe<sub>2</sub> shows a positive magnetostriction. Increasing  $H$  from zero, the magnetostriction of Ni and TbFe<sub>2</sub> both increase. When  $H > 1$  kOe, the magnetostriction of Ni is saturated at the value about  $-41$  ppm. On the contrary, the magnetostriction of TbFe<sub>2</sub> does not reach the saturation stage even though  $H = 4$  kOe. The excellent magnetostrictive properties of Ni and TbFe<sub>2</sub> are the basis for the enhancement of the ME coupling.

Figure 3(a) shows the variation of ME voltage coefficient  $\alpha_E$  under bias magnetic field  $H_{dc}$  at  $f = 1$  kHz for the Ni/PZT/TbFe<sub>2</sub> and TbFe<sub>2</sub>/PZT semiring structures. Here,  $\alpha_E$  shows strong dependence with  $H_{dc}$  that when increasing the  $H_{dc}$  value from zero,  $\alpha_E$  sharply increases to a maximum at a certain  $H_m$  and then decreases rapidly to a minimum. Although having a similar behavior, the Ni/PZT/TbFe<sub>2</sub> semiring structure shows a much higher  $\alpha_E$  than the TbFe<sub>2</sub>/PZT semiring structure.

ME voltage coefficient  $\alpha_E$  at different ac magnetic field frequencies  $f$  is also characterized. In this measurement, the

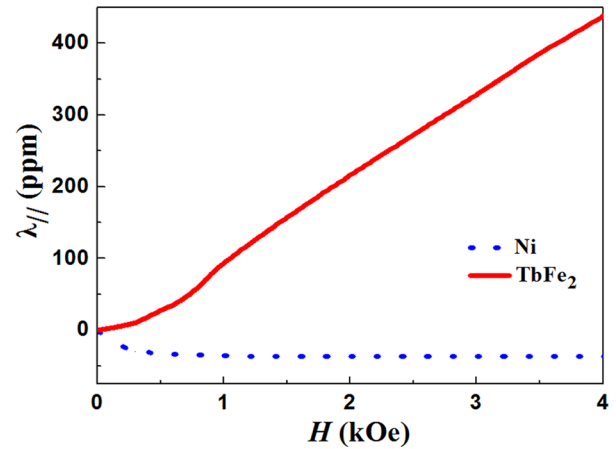


FIG. 2. The dependence of in-plane parallel magnetostriction  $\lambda_{//}$  on the applied magnetic field  $H$  for the Ni and TbFe<sub>2</sub>.

bias magnetic field  $H_{dc}$  was set to  $H_m$  and  $\alpha_E$  was measured as  $f$  varied from 1 to 100 kHz. Typical  $\alpha_E$  versus  $f$  plots for two structures are shown in Fig. 3(b). Except for the resonance region, no remarkable frequency dispersion is observed. Both of the samples show maximum  $\alpha_E$  values at the resonance frequencies. While for the Ni/PZT/TbFe<sub>2</sub> semiring structure,  $\alpha_E$  reaches a maximum value of  $40.5 \text{ V cm}^{-1} \text{ Oe}^{-1}$  at  $f = 49.4$  kHz, which is much larger than that of  $\alpha_E = 36.1 \text{ V cm}^{-1} \text{ Oe}^{-1}$  for TbFe<sub>2</sub>/PZT semiring structure at  $f = 55.1$  kHz.

In these semiring structures, ME effect is generated as a coupling of magnetic-mechanical-dielectric behavior. For the Ni/PZT/TbFe<sub>2</sub> semiring structure, when applied with the dc bias magnetic field and ac magnetic field, the outer Ni layer forms a shrinkage strain while the TbFe<sub>2</sub> insert produces an extensional strain because of their different magnetostrictive properties. These strains are then transferred to the PZT semiring. Due to the piezoelectric effect, the PZT layer induces a charge output. For the TbFe<sub>2</sub>/PZT semiring structure, only the TbFe<sub>2</sub> insert produces an extensional strain, which results in the radial and shearing deformations of the PZT semiring. Combined with the data shown in Fig. 3(b), the ME coupling is strongly influenced by the magnetostrictive properties of different materials. Obviously, due to the existence of the outer Ni layer, Ni/PZT/TbFe<sub>2</sub> semiring structure shows a better ME coupling.

Figure 4 shows representative data on radius  $R$  dependence of the resonance frequency  $f_r$  and the maximum ME

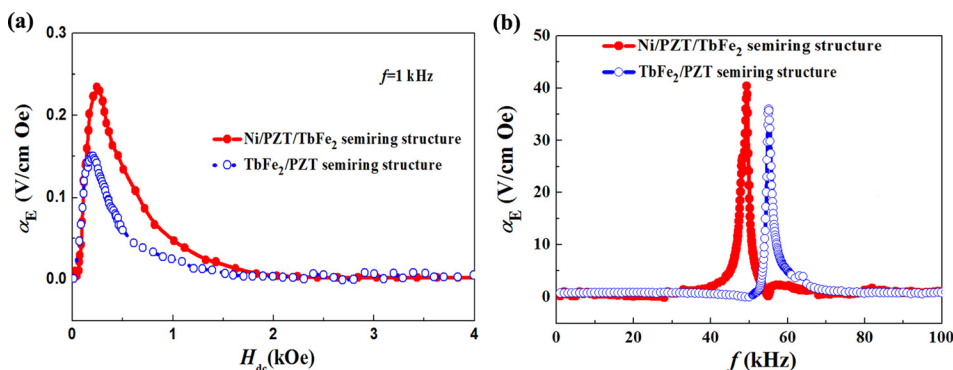


FIG. 3. (a) Bias magnetic field  $H_{dc}$  dependence of ME voltage coefficient  $\alpha_E$  at  $f = 1$  kHz, (b) ac magnetic field frequency  $f$  dependence of  $\alpha_E$  at  $H_{dc} = 180$  Oe for the Ni/PZT/TbFe<sub>2</sub> semiring structure and at  $H_{dc} = 240$  Oe for the TbFe<sub>2</sub>/PZT semiring structure. The radius  $R$  is 12.0 mm.

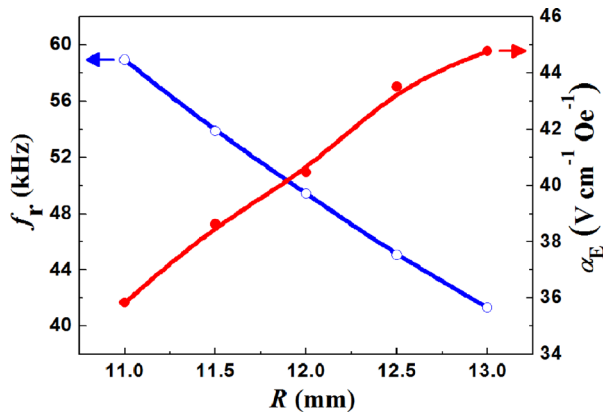


FIG. 4. The dependence of the resonance frequency  $f_r$  and the maximum ME voltage coefficient  $\alpha_E$  on radius  $R$ .

voltage coefficient  $\alpha_E$  of the Ni/PZT/TbFe<sub>2</sub> semiring structures. Increasing the radius from 11.0 mm to 13.0 mm, the  $f_r$  of Ni/PZT/TbFe<sub>2</sub> semiring structure gradually decreases from 58.9 to 41.3 kHz, while the maximum of  $\alpha_E$  increases from 35.8 to 44.8  $\text{V cm}^{-1} \text{Oe}^{-1}$ . This is because the ME coupling is affected by the curvature.<sup>18</sup> It suggests that controlled resonance frequency and maximum ME voltage coefficient can be obtained by variation of the radius of Ni/PZT/TbFe<sub>2</sub> semiring structure.

#### IV. CONCLUSIONS

ME effect of the semiring structures is investigated. The ME voltage coefficient of Ni/PZT/TbFe<sub>2</sub> semiring structure is much larger than that of TbFe<sub>2</sub>/PZT semiring structure, which confirms that the negative magnetostrictive/piezoelectric/positive magnetostrictive semiring structure possesses a stronger ME coupling. With the increase of the semiring radius, the resonance frequency gradually decreases and the maximum ME voltage coefficient increases. A giant ME voltage coefficient  $\alpha_E = 44.8 \text{ V cm}^{-1} \text{Oe}^{-1}$  is obtained when the radius is 13.0 mm. The giant ME voltage coefficient makes these semiring structures suitable for applications in magnetic field sensors and tunable frequency devices.

#### ACKNOWLEDGMENTS

This work was supported by the National Natural Science Foundation of China under Grant Nos. 51402163, 61376018, 51032003, 11274198, 51102148, and 51221291; the China Postdoctoral Science Foundation under Grant No. 2014T70075; the Fundamental Research Funds for the Central Universities under Grant No. 2015RC18; and the Fund of State Key Laboratory of Information Photonics and

Optical Communications (Beijing University of Posts and Telecommunications), China.

- <sup>1</sup>Y. K. Fetisov, A. A. Bush, K. E. Kamentsev, A. Y. Ostashchenko, and G. Srinivasan, "Ferrite-piezoelectric multilayers for magnetic field sensors," *IEEE Sens. J.* **6**, 935–938 (2006).
- <sup>2</sup>M. Fiebig, "Revival of the magnetoelectric effect," *J. Phys. D: Appl. Phys.* **38**, R123–R152 (2005).
- <sup>3</sup>C. Israel, N. D. Mathur, and J. F. Scott, "A one-cent room-temperature magnetoelectric sensor," *Nat. Mater.* **7**, 93–94 (2008).
- <sup>4</sup>P. Ravindran, R. Vidya, O. Eriksson, and H. Fjellvag, "Magnetic-instability-induced giant magnetoelectric coupling," *Adv. Mater.* **20**, 1353–1356 (2008).
- <sup>5</sup>J. Zhai, Z. Xing, S. Dong, J. Li, and D. Viehland, "Magnetoelectric laminate composites: An overview," *J. Am. Ceram. Soc.* **91**, 351–358 (2008).
- <sup>6</sup>D. A. Pan, J. Wang, Z. J. Zuo, S. G. Zhang, B. Liu, A. A. Volinsky, and L. J. Qiao, "Improved magnetoelectric performance of the Ni-P/Ni/Pb(Zr,Ti)O<sub>3</sub> cylindrical layered composites," *Appl. Phys. Lett.* **105**, 102902 (2014).
- <sup>7</sup>L. R. Xu, D. A. Pan, Z. J. Zuo, J. Wang, A. A. Volinsky, and L. J. Qiao, "Multi-electrode Pb(Zr,Ti)O<sub>3</sub>/Ni cylindrical layered magnetoelectric composite," *Appl. Phys. Lett.* **106**, 032904 (2015).
- <sup>8</sup>H. M. Wang, E. Pan, and W. Q. Chen, "Enhancing magnetoelectric effect via the curvature of composite cylinder," *J. Appl. Phys.* **107**, 093514 (2010).
- <sup>9</sup>J. Ryu, A. V. Carazo, K. Uchino, and H. E. Kim, "Magnetoelectric properties in piezoelectric and magnetostrictive laminate composites," *Jpn. J. Appl. Phys., Part 1* **40**, 4948–4951 (2001).
- <sup>10</sup>D. V. Chashin, Y. K. Fetisov, E. V. Tafintseva, and G. Srinivasan, "Magnetoelectric effects in layered samples of lead zirconium titanate and nickel films," *Solid State Commun.* **148**, 55–58 (2008).
- <sup>11</sup>M. I. Bichurin, D. A. Filippov, V. M. Petrov, V. M. Laletsin, N. Paddubnaya, and G. Srinivasan, "Resonance magnetoelectric effects in layered magnetostrictive-piezoelectric composites," *Phys. Rev. B* **68**, 132408 (2003).
- <sup>12</sup>K. Bi, Y. G. Wang, and W. Wu, "Tunable resonance frequency of magnetostrictive layered composites," *Sens. Actuators, A* **166**, 48–51 (2011).
- <sup>13</sup>C. W. Nan, "Magnetoelectric effect in composites of piezoelectric and piezomagnetic phases," *Phys. Rev. B* **50**, 6082–6088 (1994).
- <sup>14</sup>B. Cui, C. Song, H. Mao, H. Wu, F. Li, J. Peng, G. Wang, F. Zeng, and F. Pan, "Magnetoelectric coupling induced by interfacial orbital reconstruction," *Adv. Mater.* **27**, 6651–6656 (2015).
- <sup>15</sup>K. Bi, Y. G. Wang, D. A. Pan, and W. Wu, "Large magnetoelectric effect in negative magnetostrictive/piezoelectric/positive magnetostrictive laminate composites with two resonance frequencies," *Scr. Mater.* **63**, 589–592 (2010).
- <sup>16</sup>J. Y. Zhai, S. X. Dong, Z. P. Xing, J. F. Li, and D. Viehland, "Giant magnetoelectric effect in Metglas/polyvinylidene-fluoride laminates," *Appl. Phys. Lett.* **89**, 083507 (2006).
- <sup>17</sup>N. Zhang, V. M. Petrov, T. Johnson, S. K. Mandal, and G. Srinivasan, "Enhancement of magnetoelectric coupling in a piezoelectric-magnetostrictive semiring structure," *J. Appl. Phys.* **106**, 126101 (2009).
- <sup>18</sup>K. Bi, W. Wu, and Y. G. Wang, "Magnetoelectric effect in layered composites with arc shape," *Chin. Phys. B* **20**, 067503 (2011).
- <sup>19</sup>K. Bi and Y. G. Wang, "Magnetoelectric Ni-Pb(Zr,Ti)O<sub>3</sub>-Ni trilayers prepared by electroless deposition," *Solid State Commun.* **150**, 248–250 (2010).
- <sup>20</sup>K. Bi, Y. G. Wang, W. Wu, and D. A. Pan, "The large magnetoelectric effect in Ni-lead zirconium titanate-Ni trilayers derived by electroless deposition," *J. Phys. D: Appl. Phys.* **43**, 132002 (2010).
- <sup>21</sup>J. Lu, D.-A. Pan, B. Yang, and L. Qiao, "Wideband magnetoelectric measurement system with the application of a virtual multi-channel lock-in amplifier," *Meas. Sci. Technol.* **19**, 045702 (2008).